SIAM J. SCI. COMPUT.
Vol. 47, No. 6, pp. A3441–A3463

SAV-BASED ENTROPY-DISSIPATIVE SCHEMES FOR A CLASS OF KINETIC EQUATIONS*

SHIHENG ZHANG†, JIE SHEN‡, AND JINGWEI HU§

Abstract. We introduce novel entropy-dissipative numerical schemes for a class of kinetic equations, leveraging the recently introduced scalar auxiliary variable (SAV) approach. Both first and second order schemes are constructed. Since the positivity of the solution is closely related to entropy, we also propose positivity-preserving versions of these schemes to ensure robustness, which include a scheme specially designed for the Boltzmann equation and a more general scheme using Lagrange multipliers. The accuracy and provable entropy-dissipation properties of the proposed schemes are validated for both the Boltzmann equation and the Landau equation through extensive numerical examples.

Key words. entropy dissipation, positivity-preserving, mass conservation, Lagrange multiplier, Boltzmann equation, Landau equation

MSC codes. 35Q20, 82C40

DOI. 10.1137/24M1689016

1. Introduction.

We are interested in structure-preserving discretizations to the prototype kinetic equation[1] given by

$$\partial_t f = Q(f), \tag{1.1}$$

where $f = f(t, v)$ is the probability density function of time $t \geq 0$ and velocity $v \in \mathbb{R}^d$, and $Q(f)$ is the collision operator modeling particle collisions. Depending on the application, $Q(f)$ can take various forms, but they generally satisfy the following common properties:

- conservation of mass, momentum, and energy:

$$\int_{\mathbb{R}^d} Q(f)\,\mathrm{d}v = \int_{\mathbb{R}^d} Q(f) v\,\mathrm{d}v = \int_{\mathbb{R}^d} Q(f)|v|^2\,\mathrm{d}v = 0, \tag{1.2}$$

- Boltzmann's *H-theorem*:

$$\int_{\mathbb{R}^d} Q(f)\log f\,\mathrm{d}v \leq 0, \tag{1.3}$$

and the equality sign holds if and only if f becomes the *Maxwellian*:

$$M = \frac{\rho}{(2\pi T)^{d/2}} \exp\left(-\frac{|v-u|^2}{2T}\right), \tag{1.4}$$

*Submitted to the journal's Numerical Algorithms for Scientific Computing section August 29, 2024; accepted for publication (in revised form) August 28, 2025; published electronically November 11, 2025.

https://doi.org/10.1137/24M1689016

Funding: The work of first and third authors is supported by DOE DE-SC0023164. The work of third author is also partially supported by NSF DMS-2409858, and DoD MURI FA9550-24-1-0254. The work of second author is supported by National Natural Science Foundation of China under grants W2431008 and 12371409.

†Department of Applied Mathematics, University of Washington, Seattle, WA 98195 USA (shzhang3@uw.edu).

‡School of Mathematical Sciences, Eastern Institute of Technology, Ningbo, Zhejiang, 315200 People's Republic of China (jshen@eitech.edu.cn).

§Corresponding author. Department of Applied Mathematics, University of Washington, Seattle, WA 98195 USA (hujw@uw.edu).

[1]Many kinetic equations also depend on the spatial variable x. In this work, we restrict ourselves to the spatially homogeneous case, that is, $f(t, x, v)$ is assumed to be homogeneous in the x direction.

where the density ρ, bulk velocity u, and temperature T are defined as

$$\rho = \int_{\mathbb{R}^d} f \,\mathrm{d}v, \quad u = \frac{1}{\rho}\int_{\mathbb{R}^d} fv \,\mathrm{d}v, \quad T = \frac{1}{d\rho}\int_{\mathbb{R}^d} f|v-u|^2 \,\mathrm{d}v. \tag{1.5}$$

Using these properties, one can easily show that the solution to (1.1) satisfies

$$\frac{\mathrm{d}}{\mathrm{d}t}\int_{\mathbb{R}^d} f(1, v, |v|^2)^T \,\mathrm{d}v = \int_{\mathbb{R}^d} \partial_t f(1, v, |v|^2)^T \,\mathrm{d}v = \int_{\mathbb{R}^d} Q(f)(1, v, |v|^2)^T \,\mathrm{d}v = 0, \tag{1.6}$$

hence ρ, u, and T remain as constant; furthermore,

$$\frac{\mathrm{d}}{\mathrm{d}t}\int_{\mathbb{R}^d} f\log f \,\mathrm{d}v = \int_{\mathbb{R}^d} \partial_t f(\log f + 1) \,\mathrm{d}v = \int_{\mathbb{R}^d} Q(f)(\log f + 1) \,\mathrm{d}v \le 0, \tag{1.7}$$

hence the entropy $\int_{\mathbb{R}^d} f\log f \,\mathrm{d}v$ decays over time.

A large class of kinetic equations falls into the form of (1.1), including the Boltzmann equation [6], the Landau equation [18], and their simplified versions such as the Bhatnagar–Gross–Krook (BGK) model [3], the ellipsoidal-statistical BGK (ES-BGK) model [16], and the kinetic Fokker–Planck model [33], to name a few. In particular, the Boltzmann collision operator that describes neutral particle collisions is given by

$$Q_B(f)(v) = \int_{\mathbb{R}^d}\int_{S^{d-1}} B(v - v_*, \sigma)[f(v')f(v'_*) - f(v)f(v_*)] \,\mathrm{d}\sigma \,\mathrm{d}v_*, \tag{1.8}$$

where σ is a vector varying over the unit sphere S^{d-1} ($d \ge 2$), (v, v_*) and (v', v'_*) are the velocity pairs before and after a collision, related by

$$v' = \frac{v + v_*}{2} + \frac{|v - v_*|}{2}\sigma, \quad v'_* = \frac{v + v_*}{2} - \frac{|v - v_*|}{2}\sigma, \tag{1.9}$$

and the collision kernel B assumes the form

$$B(v - v_*, \sigma) = C_B|v - v_*|^\gamma b(\cos\theta), \quad \cos\theta = \frac{\sigma\cdot(v - v_*)}{|v - v_*|}, \quad -d < \gamma \le 1. \tag{1.10}$$

On the other hand, the Landau collision operator that describes charged particle collisions is given by

$$Q_L(f)(v) = \nabla_v \cdot \int_{\mathbb{R}^d} A(v - v_*)[f(v_*)\nabla_v f(v) - f(v)\nabla_{v_*} f(v_*)] \,\mathrm{d}v_*, \tag{1.11}$$

where the collision kernel A is a $d \times d$ positive semidefinite matrix given by

$$A(v - v_*) = C_L|v - v_*|^\gamma(|v - v_*|^2 I_d - (v - v_*)\otimes(v - v_*)), \quad -d \le \gamma \le 1. \tag{1.12}$$

When numerically solving (1.1), it is desirable to have a time discretization scheme that captures the entropy-decay structure (1.7) at the discrete level. We first note that this can be easily achieved via the backward Euler scheme:

$$\frac{f^{n+1} - f^n}{\Delta t} = Q(f^{n+1}), \tag{1.13}$$

which implies

$$\int_{\mathbb{R}^d} f^{n+1}\log f^{n+1} \,\mathrm{d}v - \int_{\mathbb{R}^d} f^n \log f^{n+1} \,\mathrm{d}v = \Delta t \int_{\mathbb{R}^d} Q(f^{n+1})\log f^{n+1} \,\mathrm{d}v \le 0, \tag{1.14}$$

hence

$$\int_{\mathbb{R}^d} f^{n+1} \log f^{n+1} \, \mathrm{d}v \le \int_{\mathbb{R}^d} f^n \log f^{n+1} \, \mathrm{d}v \le \int_{\mathbb{R}^d} f^n \log f^n \, \mathrm{d}v, \tag{1.15}$$

where the last inequality is due to Jensen's inequality. However, the backward Euler scheme can be extremely difficult to implement for the Boltzmann equation and Landau equation due to their nonlocal and nonlinear collision operators. On the other hand, the forward Euler scheme applied to (1.1), although simple to implement, generally cannot preserve the entropy-decay structure.[2]

Motivated by the above discussion, our goal in this work is to design entropy-dissipative schemes for general kinetic equations (1.1) that are as easily implementable as the forward Euler. This presents a significant challenge, primarily due to the inherent complexity of the collision operator which precludes the application of some well-known strategies to achieve energy stability (a property similar to entropy dissipation), such as convex splitting [11, 12, 27]. Recently, the scalar auxiliary variable (SAV) method [29] has emerged as a successful approach in various domains, notably within the contexts of gradient flows [28, 30, 7, 21]. The method has subsequently been extended to solve a variety of complex problems, such as the Schrödinger equation [1], Navier–Stokes equations [19], and Wasserstein gradient flows [35]. Given the simplicity and efficiency of the SAV method, it has also prompted extensive research beyond solving PDEs, including optimization [20, 36] and machine learning [23, 34].

This paper proposes a novel strategy to develop entropy-dissipative schemes for kinetic equations (1.1) leveraging the SAV approach. Both first and second order schemes are constructed. Since the positivity of the solution is closely related to entropy (as $\log f$ is not even defined for negative f), we also propose positivity-preserving versions of these schemes to ensure robustness, which include a scheme specially designed for the Boltzmann equation and a more general scheme using Lagrange multipliers [17, 15, 13, 2]. This latter approach has recently been applied to parabolic problems to address challenges in preserving positivity and mass conservation, as demonstrated in [31, 8].

Finally, we mention that our main focus of this work is regarding the time discretization. To simplify the presentation, we keep the velocity variable v as continuous in the following discussion. However, it should be understood that a discretization method for the collision operator is employed and we assume that this method satisfies the following properties:

- it assumes a truncation in the velocity domain: $v \in \Omega$ instead of $\mathbb{R}^d$;
- it preserves mass, momentum and energy in Ω as in (1.2);
- it satisfies the *H-theorem* in Ω as in (1.3).

There exist such methods in the literature, for example, the discrete velocity methods for the Boltzmann collision operator [10] and the Landau collision operator [9] satisfy the above assumptions. The Fourier spectral methods for the Boltzmann collision operator [25, 24, 14] and the Landau collision operator [26] coupled with the entropy fix [5] can also satisfy the above assumptions, except for momentum and energy conservation.

The rest of this paper is organized as follows. Section 2 introduces the entropy-dissipative SAV schemes. These schemes can achieve entropy dissipation but the positivity of the solution is not guaranteed. Subsequently, section 3 presents a

[2]There are some exceptions: e.g., the forward Euler for the Boltzmann equation with Maxwell collision kernel (i.e., $\gamma = 0$ in (1.10)) is readily entropy-dissipative, as proved in [32].

positivity-preserving and entropy-dissipative SAV scheme, tailored specifically for the Boltzmann equation. Section 4 introduces positivity-preserving and entropy-dissipative SAV schemes applicable to a broader class of kinetic equations. Section 5 provides a summary of the numerical schemes proposed in this paper along with their corresponding properties, and presents extensive numerical examples for the Boltzmann equation and Landau equation to demonstrate the performance of the proposed schemes. Some concluding remarks are given in section 6.

2. Entropy-dissipative SAV schemes. We define $H(t) = \int_\Omega f \log f \,\mathrm{d}v + C$, where C is a constant chosen such that $H(t) \geq H_{\min} > 0$ for all $t \geq 0$. Since entropy decreases toward a minimum (when f becomes the Maxwellian M), the lower bound of $\int_\Omega f \log f \,\mathrm{d}v$ is directly computable (i.e., $\int_\Omega M \log M \,\mathrm{d}v$). Hence determining the constant C is not difficult. We then introduce a scalar auxiliary variable (SAV) r:

$$r = \sqrt{H},$$

and rewrite (1.1) equivalently as

$$\partial_t f = \frac{r}{\sqrt{H}} Q(f), \tag{2.1}$$

$$\frac{\mathrm{d}r}{\mathrm{d}t} = \frac{1}{2\sqrt{H}} \int_\Omega \log f \partial_t f \,\mathrm{d}v, \tag{2.2}$$

where the second equation is derived by differentiating r with respect to t and applying conservation of mass.

2.1. A first order scheme. A first order numerical scheme, `SAV-1st`, for (2.1) and (2.2) can be obtained as follows:

$$\frac{f^{n+1} - f^n}{\Delta t} = \frac{r^{n+1}}{\sqrt{H^n}} Q(f^n), \tag{2.3}$$

$$\frac{r^{n+1} - r^n}{\Delta t} = \frac{1}{2\sqrt{H^n}} \int_\Omega \log f^n \frac{f^{n+1} - f^n}{\Delta t} \,\mathrm{d}v, \tag{2.4}$$

where $H^n = H(f^n) = \int_\Omega f^n \log f^n \,\mathrm{d}v + C > 0$, and $r^0 = \sqrt{H^0}$. Note that in general $r^n \neq \sqrt{H^n}$ for $n > 0$. This scheme is easy to implement. One can determine r^{n+1} by plugging (2.3) into (2.4) and then compute f^{n+1} using (2.3).

THEOREM 2.1. *The scheme* (2.3) *and* (2.4)*,* `SAV-1st`*, satisfies the following properties: for all time steps* $n \geq 0$ *and step size* $\Delta t > 0$*,*

- *it conserves mass, momentum, and energy:*

$$\int_\Omega f^{n+1}(1, v, |v|^2)^T \,\mathrm{d}v = \int_\Omega f^n (1, v, |v|^2)^T \,\mathrm{d}v;$$

- *it satisfies a modified entropy dissipation law:*

$$\tilde{H}^{n+1} - \tilde{H}^n = -(r^{n+1} - r^n)^2 + \frac{\Delta t (r^{n+1})^2}{H^n} \int_\Omega Q(f^n) \log f^n \,\mathrm{d}v \leq 0,$$

where $\tilde{H}^n = (r^n)^2$.

Proof. Conservation of mass, momentum, and energy can be easily shown by multiplying (2.3) by $(1, v, |v|^2)^T$ and integrating in v, and using that

$$\int_\Omega Q(f^n)(1, v, |v|^2)^T \,\mathrm{d}v = 0.$$

To show the entropy dissipation, we can multiply (2.3) by $\frac{r^{n+1}}{\sqrt{H^n}}\log f^n$ and integrate in v, and multiply (2.4) by $2r^{n+1}$ to obtain

$$\frac{r^{n+1}}{\sqrt{H^n}}\int_\Omega \log f^n \frac{f^{n+1}-f^n}{\Delta t}\,\mathrm{d}v = \frac{(r^{n+1})^2}{H^n}\int_\Omega Q(f^n)\log f^n\,\mathrm{d}v,$$
$$\frac{2r^{n+1}(r^{n+1}-r^n)}{\Delta t} = \frac{r^{n+1}}{\sqrt{H^n}}\int_\Omega \log f^n \frac{f^{n+1}-f^n}{\Delta t}\,\mathrm{d}v.$$

Combining these two equations together, we have

$$\frac{2r^{n+1}(r^{n+1}-r^n)}{\Delta t} = \frac{(r^{n+1})^2}{H^n}\int_\Omega Q(f^n)\log f^n\,\mathrm{d}v.$$

Noting the identity

$$2r^{n+1}(r^{n+1}-r^n) = (r^{n+1})^2 - (r^n)^2 + (r^{n+1}-r^n)^2, \tag{2.5}$$

we then have

$$(r^{n+1})^2 - (r^n)^2 + (r^{n+1}-r^n)^2 = \frac{\Delta t(r^{n+1})^2}{H^n}\int_\Omega Q(f^n)\log f^n\,\mathrm{d}v \le 0. \qquad \square$$

2.2. A second order scheme. A second order numerical scheme, `SAV-2nd`, for (2.1) and (2.2) can be constructed by extending the second order backward differentiation formula (BDF) as follows:

$$\frac{3f^{n+1}-4f^n+f^{n-1}}{2\Delta t} = \frac{r^{n+1}}{\sqrt{H^{n+1,*}}}Q(f^{n+1,*}), \tag{2.6}$$

$$\frac{3r^{n+1}-4r^n+r^{n-1}}{2\Delta t} = \frac{1}{2\sqrt{H^{n+1,*}}}\int_\Omega \log f^{n+1,*}\frac{3f^{n+1}-4f^n+f^{n-1}}{2\Delta t}\,\mathrm{d}v, \tag{2.7}$$

where $r^0=\sqrt{H^0}$ and r^1, f^1 are obtained by the first order scheme `SAV-1st`. Further, $H^{n+1,*}$ represents $H(f^{n+1,*})$, where $f^{n+1,*}$ is an explicit approximation of $f(t^{n+1})$ with an order of accuracy $\mathcal{O}(\Delta t^2)$. For example, the Adams–Bashforth extrapolation [4] can be employed for this purpose:

$$f^{n+1,*} = 2f^n - f^{n-1}.$$

THEOREM 2.2. *The scheme* (2.6) *and* (2.7), *`SAV-2nd`, satisfies the following properties: for all time steps* $n \ge 0$ *and step size* $\Delta t > 0$,

- *it conserves mass, momentum, and energy:*

$$\int_\Omega f^{n+1}(1, v, |v|^2)^T\,\mathrm{d}v = \int_\Omega f^n(1, v, |v|^2)^T\,\mathrm{d}v;$$

- *it satisfies a modified entropy dissipation law:*

$$\tilde{H}^{n+1} - \tilde{H}^n = -\frac{1}{2}(r^{n+1}-2r^n+r^{n-1})^2 + \frac{\Delta t(r^{n+1})^2}{H^{n+1,*}}\int_\Omega Q(f^{n+1,*})\log f^{n+1,*}\,\mathrm{d}v \le 0,$$

where $\tilde{H}^n = \frac{1}{2}(r^n)^2 + \frac{1}{2}(2r^n - r^{n-1})^2$.

Proof. Conservation of mass, momentum, and energy can be easily shown by multiplying (2.6) by $(1, v, |v|^2)^T$ and integrating in v, and using that

$$\int_\Omega Q(f^{n+1,*})(1, v, |v|^2)^T \, \mathrm{d}v = 0.$$

To show the entropy dissipation, we multiply (2.6) by $\frac{r^{n+1}}{\sqrt{H^{n+1,*}}} \log f^{n+1,*}$ and integrate in v, multiply (2.7) by $2r^{n+1}$ to obtain

$$\frac{2r^n(3r^{n+1} - 4r^n + r^{n-1})}{2\Delta t} = \frac{(r^{n+1})^2}{H^{n+1,*}} \int_\Omega Q(f^{n+1,*}) \log f^{n+1,*} \, \mathrm{d}v \le 0.$$

Using the identity

$$\begin{aligned} 2r^{n+1}(3r^{n+1} - 4r^n + r^{n-1}) = {} & (r^{n+1})^2 + (2r^{n+1} - r^n)^2 + (r^{n+1} - 2r^n + r^{n-1})^2 \\ & - (r^n)^2 - (2r^n - r^{n-1})^2, \end{aligned} \tag{2.8}$$

we obtain the desired inequality. ∎

Remark 2.3. A second order scheme based on the Crank–Nicolson method can also be constructed:

$$\frac{f^{n+1} - f^n}{\Delta t} = \frac{r^{n+1} + r^n}{2\sqrt{H^{n+1/2,*}}} Q(f^{n+1/2,*}), \tag{2.9}$$

$$\frac{r^{n+1} - r^n}{\Delta t} = \frac{1}{2\sqrt{H^{n+1/2,*}}} \int_\Omega \log f^{n+1/2,*} \frac{f^{n+1} - f^n}{\Delta t} \, \mathrm{d}v, \tag{2.10}$$

where $f^{n+1/2,*}$ represents any explicit $\mathcal{O}(\Delta t^2)$ approximation to $f(t^{n+1/2})$. This scheme satisfies the same properties as Theorem 2.2, except that the entropy dissipation has a different form:

$$(r^{n+1})^2 - (r^n)^2 = \frac{\Delta t (r^{n+1} + r^n)^2}{4H^{n+1/2,*}} \int_\Omega Q(f^{n+1/2,*}) \log f^{n+1/2,*} \, \mathrm{d}v \le 0.$$

3. A positivity-preserving and entropy-dissipative SAV scheme for the Boltzmann equation. Since f is the probability density function, so it should satisfy $f \ge 0$. In this section, we use the Boltzmann collision operator (1.8) as an example to show how to modify the scheme `SAV-1st` in the last section to preserve positivity. First note that we can write $Q_B(f)$ as

$$Q_B(f) = Q_B^+(f) - Q_B^-(f) f, \tag{3.1}$$

with

$$Q_B^+(f)(v) = \int_\Omega \int_{S^{d-1}} B(v - v_*, \sigma) f(v') f(v'_*) \, \mathrm{d}\sigma \, \mathrm{d}v_* \ge 0, \tag{3.2}$$

$$Q_B^-(f)(v) = \int_\Omega \int_{S^{d-1}} B(v - v_*, \sigma) f(v_*) \, \mathrm{d}\sigma \, \mathrm{d}v_* \ge 0. \tag{3.3}$$

We propose a first order stabilized scheme with positivity-preserving property, `SAV-1st-P-B`, as follows

$$\frac{f^{n+1} - f^n}{\Delta t} = \frac{r^{n+1}}{\sqrt{H^n}} Q_B(f^n) + \beta f^n - \beta f^{n+1}, \tag{3.4}$$

$$\frac{r^{n+1} - r^n}{\Delta t} = \frac{1}{2\sqrt{H^n}} \int_\Omega \log f^n \frac{f^{n+1} - f^n}{\Delta t} \, \mathrm{d}v, \tag{3.5}$$

where the constant β is a stabilizing constant, chosen such that $\beta \geq \frac{r^0}{\sqrt{H_{\min}}} \max Q_B^-(f) \geq 0$. The definition of $Q_B^-(f)$ implies that

$$Q_B^-(f) \leq \rho \max_{v,v_* \in \Omega} \int_{S^{d-1}} B(v - v_*, \sigma) \, \mathrm{d}\sigma.$$

Since ρ remains constant and the velocity domain has been truncated, the upper bound of $Q_B^-(f)$ is not difficult to obtain.

THEOREM 3.1. *The scheme* (3.4) *and* (3.5), `SAV-1st-P-B`, *satisfies the following properties: for all time step* $n \geq 0$ *and step size* $\Delta t > 0$,

- *it preserves the positivity of the solution, i.e.,* $f^n \geq 0$, *provided initially* $f^0 \geq 0$;
- *it conserves mass, momentum, and energy:*

$$\int_\Omega f^{n+1}(1, v, |v|^2)^T \, \mathrm{d}v = \int_\Omega f^n(1, v, |v|^2)^T \, \mathrm{d}v;$$

- *it satisfies a modified entropy dissipation law:*

$$\tilde{H}^{n+1} - \tilde{H}^n = -(r^{n+1} - r^n)^2 + \frac{\Delta t (r^{n+1})^2}{(1 + \beta \Delta t) H^n} \int_\Omega Q_B(f^n) \log f^n \, \mathrm{d}v \leq 0,$$

where $\tilde{H}^n = (r^n)^2$.

Proof. To show the positivity of f^n, we first rewrite the (3.4) as

$$\begin{aligned} \frac{f^{n+1} - f^n}{\Delta t} &= \frac{r^{n+1}}{\sqrt{H^n}} \left(Q_B^+(f^n) - Q_B^-(f^n) f^n \right) + \beta f^n - \beta f^{n+1} \\ &= \frac{r^{n+1}}{\sqrt{H^n}} Q_B^+(f^n) + \left(\beta - \frac{r^{n+1}}{\sqrt{H^n}} Q_B^-(f^n) \right) f^n - \beta f^{n+1}, \end{aligned} \tag{3.6}$$

hence,

$$(1 + \Delta t \beta) f^{n+1} = \Delta t \frac{r^{n+1}}{\sqrt{H^n}} Q_B^+(f^n) + \left(1 + \Delta t \left(\beta - \frac{r^{n+1}}{\sqrt{H^n}} Q_B^-(f^n) \right) \right) f^n. \tag{3.7}$$

Rewriting (3.4) alternatively as

$$\left(\frac{1}{\Delta t} + \beta \right) \left(f^{n+1} - f^n \right) = \frac{r^{n+1}}{\sqrt{H^n}} Q_B(f^n), \tag{3.8}$$

and plugging (3.8) into (3.5), we can obtain:

$$r^{n+1} = \left(1 - \frac{\Delta t}{2 H^n (1 + \Delta t \beta)} \int_\Omega Q_B(f^n) \log f^n \, \mathrm{d}v \right)^{-1} r^n. \tag{3.9}$$

Since $H^n > 0$, $1 + \Delta t \beta > 0$, and $\int Q_B(f^n) \log f^n \, \mathrm{d}v \leq 0$ (H-theorem), the second term in the parentheses above is non-negative. Therefore, the entire term in the parentheses is ≥ 1. This implies that $0 \leq r^{n+1} \leq r^n$. By the choice of β, we guarantee that

$$\beta \geq \frac{r^0}{\sqrt{H_{\min}}} \max Q_B^-(f) \geq \frac{r^{n+1}}{\sqrt{H^n}} Q_B^-(f^n).$$

Using this in (3.7), we see that $f^{n+1} \geq 0$ if $f^n \geq 0$.

Conservation of mass, momentum, and energy is immediate by multiplying (3.4) by $(1, v, |v|^2)^T$ and integrating in v.

To show the entropy dissipation, we can multiply (3.8) by $\frac{r^{n+1}}{\sqrt{H^n}}\log f^n$ and integrate in v, and multiply (3.5) by $2r^{n+1}$ to obtain

$$\left(\frac{1}{\Delta t}+\beta\right)\frac{r^{n+1}}{\sqrt{H^n}}\int_\Omega \log f^n\left(f^{n+1}-f^n\right)\mathrm{d}v=\frac{(r^{n+1})^2}{H^n}\int_\Omega Q_B(f^n)\log f^n\,\mathrm{d}v,$$
$$\frac{2r^{n+1}(r^{n+1}-r^n)}{\Delta t}=\frac{r^{n+1}}{\sqrt{H^n}}\int_\Omega \log f^n\frac{f^{n+1}-f^n}{\Delta t}\,\mathrm{d}v.$$

Combining the two equations together, we have

$$2r^{n+1}(r^{n+1}-r^n)=\left(\frac{1}{\Delta t}+\beta\right)^{-1}\frac{(r^{n+1})^2}{H^n}\int_\Omega Q_B(f^n)\log f^n\,\mathrm{d}v.$$

Using the identity (2.5) together with $\beta\geq 0$, we have

$$(r^{n+1})^2-(r^n)^2+(r^{n+1}-r^n)^2=\left(\frac{1}{\Delta t}+\beta\right)^{-1}\frac{(r^{n+1})^2}{H^n}\int_\Omega Q_B(f^n)\log f^n\,\mathrm{d}v\leq 0.\quad\square$$

4. Positivity-preserving schemes for general kinetic equations. The scheme introduced in section 3 is designed for the Boltzmann equation and is limited to first order. In this section, we construct positivity-preserving and entropy-dissipative SAV schemes that work for general kinetic equations (1.1), leveraging the optimization techniques. We will achieve this in two steps. The first version focuses on restoring the positivity without mass conservation; and the second version can achieve both positivity and mass conservation.

4.1. Positivity-preserving schemes without mass conservation.

4.1.1. A first order scheme. To guarantee that f remains positive, we introduce a Lagrange multiplier function, $\lambda(t,v)$, and consider the extended system with the Karush–Kuhn–Tucker (KKT) conditions:

$$\partial_t f-Q(f)=\lambda, \tag{4.1}$$
$$\lambda\geq 0,\quad f\geq 0,\quad \lambda f=0. \tag{4.2}$$

A first order operator splitting scheme [8] with SAV and Lagrange multiplier, `SAV-1st-L`, is given as follows:

Step 1 (prediction): solve $\tilde{f}^{n+1}$ from

$$\frac{\tilde{f}^{n+1}-f^n}{\Delta t}=\frac{r^{n+1}}{\sqrt{H^n}}Q(f^n), \tag{4.3}$$
$$\frac{r^{n+1}-r^n}{\Delta t}=\frac{1}{2\sqrt{H^n}}\int_\Omega \log f^n\frac{\tilde{f}^{n+1}-f^n}{\Delta t}\,\mathrm{d}v. \tag{4.4}$$

Step 2 (correction): solve (f^{n+1},λ^{n+1}) from

$$\frac{f^{n+1}(v)-\tilde{f}^{n+1}(v)}{\Delta t}=\lambda^{n+1}(v), \tag{4.5}$$
$$\lambda^{n+1}(v)\geq 0,\quad f^{n+1}(v)\geq 0,\quad \lambda^{n+1}(v)f^{n+1}(v)=0. \tag{4.6}$$

The equations in the prediction step is the same as the scheme `SAV-1st`, hence can be solved directly and enjoy the entropy-decay property. A notable characteristic of the equations in the correction step is their solvability on a point-wise basis, as described below:

$$\left(f^{n+1}(v),\lambda^{n+1}(v)\right)=\begin{cases}\left(\tilde{f}^{n+1}(v),0\right) & \text{if } \tilde{f}^{n+1}(v)\geq 0\\ \left(0,-\frac{\tilde{f}^{n+1}(v)}{\Delta t}\right) & \text{otherwise}\end{cases},\quad \forall\ v\in\Omega. \tag{4.7}$$

THEOREM 4.1. *The scheme* (4.3)–(4.6), *`SAV-1st-L`, satisfies the following properties: for all time steps* $n\geq 0$ *and step size* $\Delta t>0$,

- *it preserves the positivity of the solution, i.e.,* $f^n\geq 0$;
- *it satisfies a modified entropy dissipation law:*

$$\tilde{H}^{n+1}-\tilde{H}^n=-(r^{n+1}-r^n)^2+\frac{\Delta t(r^{n+1})^2}{H^n}\int_\Omega Q(f^n)\log f^n\,\mathrm{d}v\leq 0,$$

where $\tilde{H}^n=(r^n)^2$.

Proof. It is clear that $f^n\geq 0$ for all n. As for the modified entropy dissipation, it can be established following a similar approach to that detailed in Theorem 2.1. ∎

Remark 4.2. We can also require that the solution is bounded away from 0 for a prescribed ϵ by substituting the optimality condition (4.6) with

$$\lambda^{n+1}(v)\geq 0,\quad f^{n+1}(v)\geq\epsilon,\quad \lambda^{n+1}(v)(f^{n+1}(v)-\epsilon)=0. \tag{4.8}$$

4.1.2. A second order scheme. A second order scheme with SAV and Lagrange multiplier, `SAV-2nd-L`, can also be constructed with the second order BDF and Adams–Bashforth extrapolation:

Step 1 (prediction): solve $\tilde{f}^{n+1}$ from

$$\frac{3\tilde{f}^{n+1}-4f^n+f^{n-1}}{2\Delta t}=\frac{r^{n+1}}{\sqrt{H^{n+1,*}}}Q(f^{n+1,*}), \tag{4.9}$$

$$\frac{3r^{n+1}-4r^n+r^{n-1}}{2\Delta t}=\frac{1}{2\sqrt{H^{n+1,*}}}\int_\Omega\log f^{n+1,*}\frac{3\tilde{f}^{n+1}-4f^n+f^{n-1}}{2\Delta t}\,\mathrm{d}v. \tag{4.10}$$

Step 2 (correction): solve (f^{n+1},λ^{n+1}) from

$$\frac{3f^{n+1}(v)-3\tilde{f}^{n+1}(v)}{2\Delta t}=\lambda^{n+1}(v), \tag{4.11}$$

$$\lambda^{n+1}(v)\geq 0,\quad f^{n+1}(v)\geq 0,\quad \lambda^{n+1}(v)f^{n+1}(v)=0. \tag{4.12}$$

Note that the Adams–Bashforth extrapolation can not preserve positivity, we need to modify it with

$$f^{n+1,*}=\begin{cases}2f^n-f^{n-1}, & \text{if } f^n\geq f^{n-1},\\ \frac{1}{2/f^n-1/f^{n-1}}, & \text{otherwise.}\end{cases} \tag{4.13}$$

The steps (4.11) to (4.12) can be solved in a similar way as in the first order case:

$$\left(f^{n+1}(v),\lambda^{n+1}(v)\right)=\begin{cases}\left(\tilde{f}^{n+1}(v),0\right) & \text{if } \tilde{f}^{n+1}(v)\geq 0\\ \left(0,-\frac{3\tilde{f}^{n+1}(v)}{2\Delta t}\right) & \text{otherwise}\end{cases},\quad \forall\ v\in\Omega. \tag{4.14}$$

THEOREM 4.3. *The scheme* (4.9)–(4.12), `SAV-2nd-L`, *satisfies the following properties: for all time steps* $n \geq 0$ *and step size* $\Delta t > 0$,

- *it preserves the positivity of the solution, i.e.,* $f^n \geq 0$;
- *it satisfies a modified entropy dissipation law:*

$$\tilde{H}^{n+1} - \tilde{H}^n = -\frac{1}{2}(r^{n+1} - 2r^n + r^{n-1})^2 + \frac{\Delta t (r^{n+1})^2}{H^{n+1,*}} \int_\Omega Q(f^{n+1,*}) \log f^{n+1,*} \, \mathrm{d}v \leq 0,$$

where $\tilde{H}^n = \frac{1}{2}(r^n)^2 + \frac{1}{2}(2r^n - r^{n-1})^2$.

Proof. It is clear that $f^n \geq 0$ for all n. The proof for the modified entropy dissipation follows from a similar approach to that detailed in Theorem 2.2. ∎

Remark 4.4. We note that while a second-order Crank–Nicolson SAV scheme was introduced in Remark 2.3, extending it to achieve positivity preservation using the Lagrange multiplier approach presented in this section poses a significant challenge. The Crank–Nicolson method is centered at $t^{n+1/2}$, meaning that a consistent Lagrange multiplier correction would naturally enforce positivity at an intermediate stage like $f^{n+1/2,*}$. However, ensuring $f^{n+1/2,*} \geq 0$ does not guarantee that the final solution f^{n+1} will be non-negative. For this reason, our second-order positivity-preserving schemes are based on the BDF method.

4.2. Positivity-preserving schemes with mass conservation. The correction steps (4.7) and (4.14) are equivalent to the cutoff strategy [22], which similarly encounter issues with mass conservation. For instance, we observe from (4.5) that

$$\int_\Omega f^{n+1}(v) \, \mathrm{d}v - \int_\Omega \tilde{f}^{n+1}(v) \, \mathrm{d}v = \int_\Omega \Delta t \lambda^{n+1}(v) \, \mathrm{d}v \geq 0,$$

which suggests an increase in mass.

To enforce the mass conservation, we introduce an additional Lagrange multiplier, ξ^{n+1}, which is independent of the velocity variable. This new multiplier aims to ensure mass conservation during the correction step. A first order scheme that preserves positivity and mass conservation, `SAV-1st-LM`, is given as follows:

Step 1 (prediction): solve $\tilde{f}^{n+1}$ from

$$\frac{\tilde{f}^{n+1} - f^n}{\Delta t} = \frac{r^{n+1}}{\sqrt{H^n}} Q(f^n), \tag{4.15}$$

$$\frac{r^{n+1} - r^n}{\Delta t} = \frac{1}{2\sqrt{H^n}} \int_\Omega \log f^n \frac{\tilde{f}^{n+1} - f^n}{\Delta t} \, \mathrm{d}v. \tag{4.16}$$

Step 2 (correction): solve $(f^{n+1}, \lambda^{n+1}, \xi^{n+1})$ from

$$\frac{f^{n+1}(v) - \tilde{f}^{n+1}(v)}{\Delta t} = \lambda^{n+1}(v) + \xi^{n+1}, \tag{4.17}$$

$$\lambda^{n+1}(v) \geq 0, \quad f^{n+1}(v) \geq 0, \quad \lambda^{n+1}(v) f^{n+1}(v) = 0, \tag{4.18}$$

$$\int_\Omega f^{n+1}(v) \, \mathrm{d}v = \int_\Omega f^n(v) \, \mathrm{d}v. \tag{4.19}$$

In order to solve the correction step, we rewrite (4.17) in the following equivalent form

$$\frac{f^{n+1}(v) - \left(\tilde{f}^{n+1}(v) + \Delta t \xi^{n+1}\right)}{\Delta t} = \lambda^{n+1}(v). \tag{4.20}$$

Hence, assuming ξ^{n+1} is known, (4.18) and (4.20) can be solved point-wise similarly as in the previous subsection:

(4.21)
$$\left(f^{n+1}(v),\lambda^{n+1}(v)\right)=\begin{cases}\left(\tilde f^{n+1}(v)+\Delta t\xi^{n+1},0\right) & \text{if } \tilde f^{n+1}(v)+\Delta t\xi^{n+1}\ge 0\\ \left(0,-\frac{\tilde f^{n+1}(v)+\Delta t\xi^{n+1}}{\Delta t}\right) & \text{otherwise}\end{cases},\ \forall\ v\in\Omega.$$

It remains to determine ξ^{n+1}. We find from (4.19) and (4.20) that

$$\int_\Omega \tilde f^{n+1}+\Delta t\xi^{n+1}\,\mathrm{d}v=\int_\Omega f^n\,\mathrm{d}v-\int_\Omega \Delta t\lambda^{n+1}\,\mathrm{d}v,$$

which, thanks to (4.21), can be rewritten as

$$\int_{v\in\Omega\text{ s.t. }0<\tilde f^{n+1}(v)+\Delta t\xi^{n+1}} \tilde f^{n+1}+\Delta t\xi^{n+1}\,\mathrm{d}v=\int_\Omega f^n\,\mathrm{d}v. \tag{4.22}$$

Hence, ξ^{n+1} is a solution to the nonlinear algebraic equation

$$F(\xi)=\int_{v\in\Omega\text{ s.t. }0<\tilde f^{n+1}(v)+\Delta t\xi} \tilde f^{n+1}+\Delta t\xi\,\mathrm{d}v-\int_\Omega f^n\,\mathrm{d}v=0. \tag{4.23}$$

Since $F'(\xi)$ may not exist and is difficult to compute if it exists, instead of the Newton iteration, we can use the following secant method:

$$\xi_{k+1}=\xi_k-\frac{F(\xi_k)(\xi_k-\xi_{k-1})}{F(\xi_k)-F(\xi_{k-1})}. \tag{4.24}$$

Since ξ^{n+1} is an approximation to zero, and it can be shown that $\xi^{n+1}\le 0$ if we add (4.17) to (4.15) and take the integration, we can choose $\xi_0=0$ and $\xi_1=-O(\Delta t)$. Once ξ^{n+1} is known, we can update $\left(f^{n+1}(v),\lambda^{n+1}(v)\right)$ with (4.21).

A second order scheme, `SAV-2nd-LM`, can be constructed as follows:

Step 1 (prediction): solve $\tilde f^{n+1}$ from

$$\frac{3\tilde f^{n+1}-4f^n+f^{n-1}}{2\Delta t}=\frac{r^{n+1}}{\sqrt{H^{n+1,*}}}Q(f^{n+1,*}), \tag{4.25}$$

$$\frac{3r^{n+1}-4r^n+r^{n-1}}{2\Delta t}=\frac{1}{2\sqrt{H^{n+1,*}}}\int_\Omega \log f^{n+1,*}\frac{3\tilde f^{n+1}-4f^n+f^{n-1}}{2\Delta t}\,\mathrm{d}v. \tag{4.26}$$

Step 2 (correction): solve $\left(f^{n+1},\lambda^{n+1},\xi^{n+1}\right)$ from

$$\frac{3f^{n+1}(v)-3\tilde f^{n+1}(v)}{2\Delta t}=\lambda^{n+1}(v)+\xi^{n+1}, \tag{4.27}$$

$$\lambda^{n+1}(v)\ge 0,\quad f^{n+1}(v)\ge 0,\quad \lambda^{n+1}(v)f^{n+1}(v)=0, \tag{4.28}$$

$$\int_\Omega f^{n+1}(v)\,\mathrm{d}v=\int_\Omega f^n(v)\,\mathrm{d}v, \tag{4.29}$$

where

$$f^{n+1,*}=\begin{cases}2f^n-f^{n-1}, & \text{if } f^n\ge f^{n-1},\\ \frac{1}{2/f^n-1/f^{n-1}}, & \text{otherwise.}\end{cases} \tag{4.30}$$

The first order scheme (4.15)–(4.19), `SAV-1st-LM`, and the second order scheme (4.25)–(4.29), `SAV-2nd-LM`, satisfy the same properties as in Theorem 4.1 and Theorem 4.3, respectively. In addition, they both conserve mass:

$$\int_\Omega f^{n+1}\,\mathrm{d}v = \int_\Omega f^n\,\mathrm{d}v.$$

Remark 4.5. The schemes introduced above only conserve mass. While conservation of momentum and energy could, in principle, be achieved by introducing additional Lagrange multipliers, this approach would lead to a coupled nonlinear system for the Lagrange multipliers, and complicate the solution process. Therefore, we do not pursue momentum and energy conservation here.

5. Numerical examples. In this section, we present several numerical results to demonstrate the properties of the proposed schemes.

For readers' convenience, we first provide a summary on the properties of the proposed numerical schemes in this paper. In Table 1, "Conservation" refers to conservation of mass, momentum, and energy (unless otherwise specified); "modified entropy" could take different forms for different schemes; whenever a second order scheme is indicated, it means that the scheme satisfies the same properties as the first order scheme in the same row.

In our numerical experiments below, we focus our attention on the Boltzmann collision operator (1.8) and the Landau collision operator (1.11). For velocity domain discretization, we employ the Fourier spectral methods [24, 26] for these operators. Although the Fourier spectral methods do not strictly satisfy the three conditions listed in the Introduction, their high accuracy ensures that the error from velocity discretization is negligible compared to that from time discretization, allowing us to conduct a meaningful validation of the proposed schemes. For all of the following tests, we assume the two-dimensional velocity domain $\Omega = [-L, L)^2$ and use $N = 64$ Fourier modes in each dimension. The model specific parameters are chosen as

- Boltzmann: collision kernel $B = \frac{1}{2\pi}, L = (3\sqrt{2}+1)S/2$;
- Landau: collision kernel $A = \frac{1}{16}(|v-v_*|^2 I_2 - (v-v_*)\otimes(v-v_*)), L = 2S$.

The value of S will be specified in each test.

For all SAV-based schemes in the following, we set the constant $C = 10$ to ensure that $H(f) = \int_\Omega f \log f\,\mathrm{d}v + C > 0$. For `sav-1st-LM` and `sav-2nd-LM`, our implementation ensures that $f^n \geq \epsilon = 10^{-16}$, as described in (4.8), to maintain well-defined logarithmic term, $\log f^n$, throughout the computational process. To clarify the terminology used in the following numerical experiments, we recall the definitions of the

TABLE 1
Properties of the proposed schemes.

Scheme	Conservation	Modified entropy decay	Positivity	Second Order
`SAV-1st` (2.3) and (2.4)	yes	yes	no	`SAV-2nd` (2.6) and (2.7)
`SAV-1st-P-B` (3.4) and (3.5) only for Boltzmann	yes	yes	yes	no
`SAV-1st-L` (4.3)–(4.6)	no	yes	yes	`SAV-2nd-L` (4.9)–(4.12)
`SAV-1st-LM` (4.15)–(4.19)	only mass	yes	yes	`SAV-2nd-LM` (4.25)–(4.29)

entropies. The modified entropy for the SAV-based schemes is $(r^n)^2$ for first order schemes and $\frac{1}{2}(r^n)^2 + \frac{1}{2}(r^n - r^{n-1})^2$ for second order schemes. The actual entropy at time t_n is $H^n = H(f^n)$, where f^n is the numerical solution. The entropy of the analytical solution at time t_n is $H(f(t_n))$, with $f(t_n)$ being the analytical solution.

5.1. Test case 1: BKW solution. The BKW solution is one of the few analytical solutions for the Boltzmann/Landau equation. When $d = 2$, it is given by

$$f(t,v) = \frac{1}{2\pi K} \exp\left(-\frac{|v|^2}{2K}\right)\left(\frac{2K-1}{K} + \frac{1-K}{2K^2}|v|^2\right), \quad K = 1 - \exp(-t/8)/2. \tag{5.1}$$

We take $t_0 = 0.5$ as the initial time and set $S = 3.3$. Note that the same solution works for both Boltzmann and Landau for the aforementioned collision kernels.

5.1.1. Convergence tests. We first perform a convergence analysis to assess the order of the `SAV-1st`, `SAV-2nd`, `SAV-1st-LM`, and `SAV-2nd-LM` schemes. We measure the relative L_∞ error between the numerical solution and the analytic solution at the final time $t_{\text{end}} = 0.6$.

For the Boltzmann equation, time step sizes are set to $\Delta t = \{0.02, 0.01, 0.005, 0.0025\}$, while for the Landau equation, much smaller steps of $\Delta t = \{0.002, 0.001, 0.0005, 0.00025\}$ are used. The results for the Boltzmann equation are shown in Figures 1a and 1b, and those for the Landau equation are shown in Figures 1c and 1d. The first and second order convergence are clearly observed.

Note that the time steps for the Landau equation in Figures 1c and 1d are chosen to be small enough such that the positivity correction (hence mass conservation correction) is never triggered in `SAV-1st-LM` and `SAV-2nd-LM`. To further demonstrate the strength of these schemes, we choose larger time step sizes of $\Delta t = \{0.02, 0.01, 0.005, 0.0025\}$ and rerun the same test. The results are shown in Figures 1e and 1f. In this case, `SAV-1st` and `SAV-2nd` result in negative values, causing the simulation to fail. In contrast, `SAV-1st-LM` and `SAV-2nd-LM` execute successfully and still demonstrate the expected convergence rates, highlighting their robustness under challenging conditions.

5.1.2. Conservation properties. To examine the conservation properties of the `SAV-1st-LM` and `SAV-2nd-LM` schemes, we plot in Figure 2 the evolution of the absolute errors in the conserved moments: mass $\int_\Omega f \, \mathrm{d}v$, momentum (first component) $\int_\Omega f v_1 \, \mathrm{d}v$, and energy $\int_\Omega f|v|^2 \, \mathrm{d}v$, relative to their initial values. This test is performed for the Landau equation with larger time step sizes $\Delta t = \{0.02, 0.01, 0.005, 0.0025\}$.

The top panels, Figure 2a and 2b, show the error in mass. For all tested time step sizes, the errors remain at the level of machine precision, fluctuating around 10^{-14}. This confirms that the Lagrange multiplier approach rigorously enforces mass conservation throughout the simulation, as intended by the scheme's design. Although the schemes do not explicitly enforce momentum and energy conservation, Figure 2c and 2d and Figure 2e and 2f also demonstrate excellent conservation properties.

5.1.3. Entropy evolution. We then focus on the entropy evolution of the schemes `SAV-1st-LM` and `SAV-2nd-LM` for both the Boltzmann equation and Landau equation.

Figure 3 showcases the results for the Boltzmann equation. The top four figures are obtained using `SAV-1st-LM`, while the bottom four figures are obtained using `SAV-2nd-LM`. These figures demonstrate that both methods accurately predict the solution, with the actual entropy closely matching the analytical entropy across all time steps. For larger time step sizes, the modified entropy exhibits a faster decay

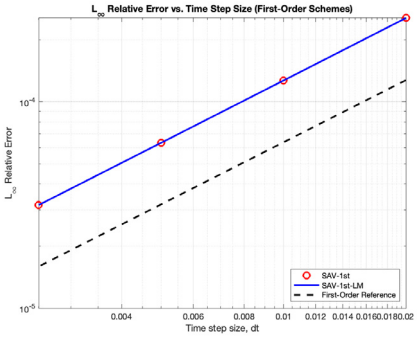

(a) Boltzmann equation: error versus time step size for `SAV-1st` and `SAV-1st-LM`.

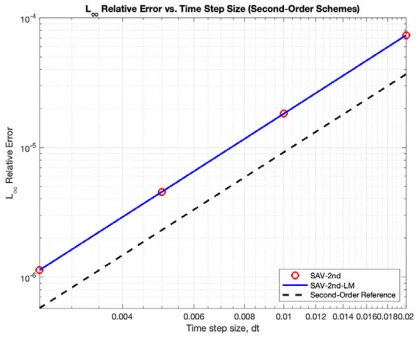

(b) Boltzmann equation: error versus time step size for `SAV-2nd` and `SAV-2nd-LM`.

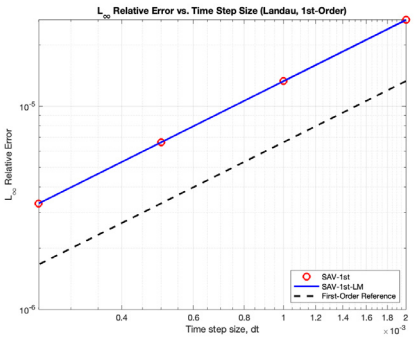

(c) Landau equation: error versus smaller time step size for `SAV-1st` and `SAV-1st-LM`.

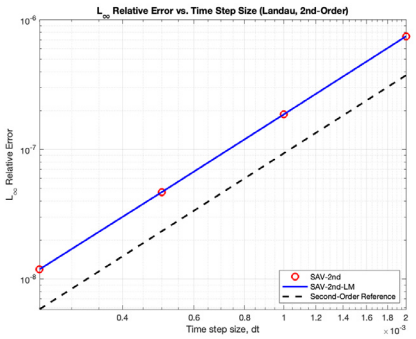

(d) Landau equation: error versus smaller time step size for `SAV-2nd` and `SAV-2nd-LM`.

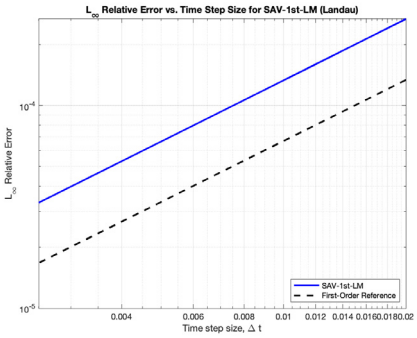

(e) Landau equation: error versus larger time step size for `SAV-1st-LM`.

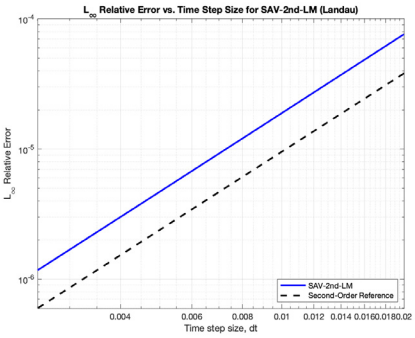

(f) Landau equation: error versus larger time step size for `SAV-2nd-LM`.

FIG. 1. *Convergence tests of the* `SAV-1st`*,* `SAV-2nd`*,* `SAV-1st-LM`*, and* `SAV-2nd-LM` *schemes for the Boltzmann equation and Landau equation.*

compared to the actual entropy, but the actual entropy consistently aligns closely with the entropy of the analytical solution. In fact, for all the results presented, the positivity and mass conservation correction is never triggered, so the results are equivalent to those obtained by `SAV-1st` and `SAV-2nd`.

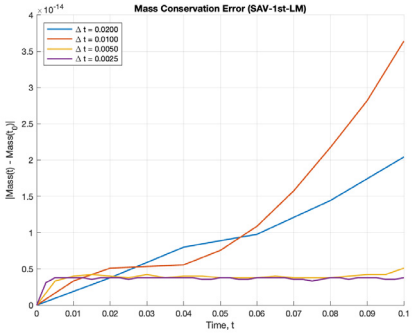

(a) Mass error (`SAV-1st-LM`).

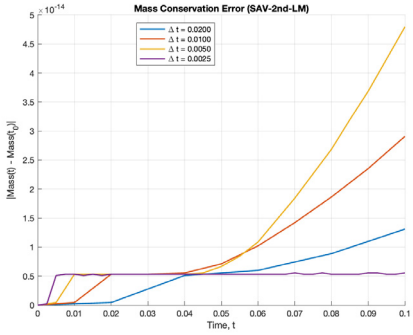

(b) Mass error (`SAV-2nd-LM`).

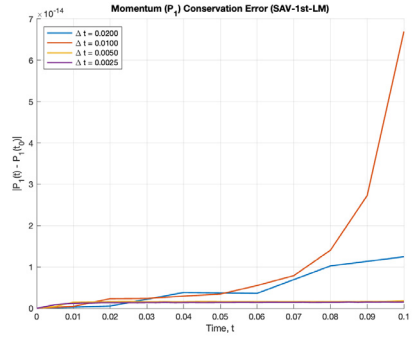

(c) Momentum error (`SAV-1st-LM`).

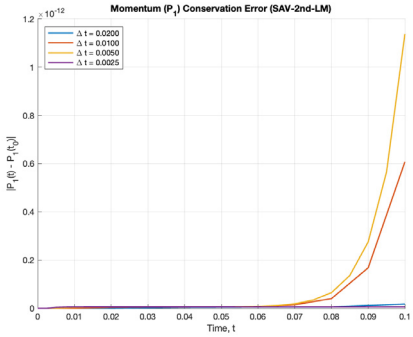

(d) Momentum error (`SAV-2nd-LM`).

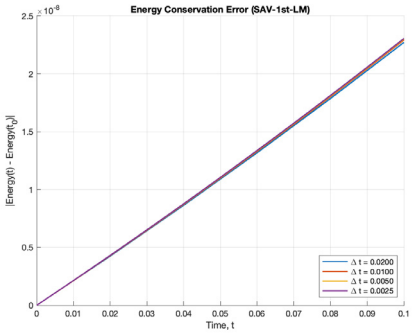

(e) Energy error (`SAV-1st-LM`).

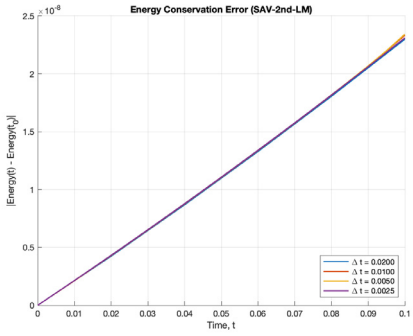

(f) Energy error (`SAV-2nd-LM`).

FIG. 2. *Time evolution of the errors in mass, momentum, and energy of the* `SAV-1st-LM` *(left column) and* `SAV-2nd-LM` *(right column) schemes for the Landau equation with different time step sizes.*

Figure 4 showcases the results for the Landau equation. The top four figures are obtained using `SAV-1st-LM`, while the bottom four figures are obtained using `SAV-2nd-LM`. It is noteworthy that whenever the modified entropy deviates from the

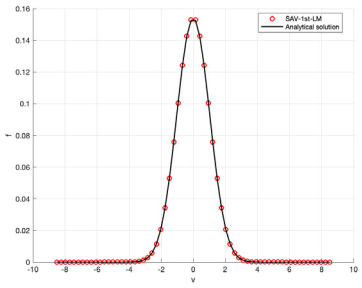

(a) f at $t_{\text{end}} = 10.5$ with $\Delta t = 0.2$.

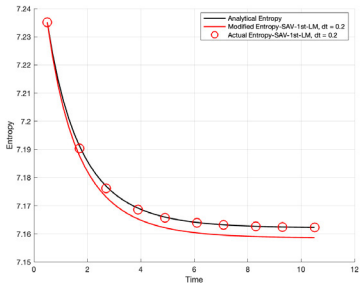

(b) Entropy evolution with $\Delta t = 0.2$.

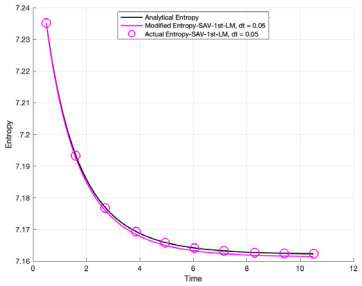

(c) Entropy evolution with $\Delta t = 0.05$.

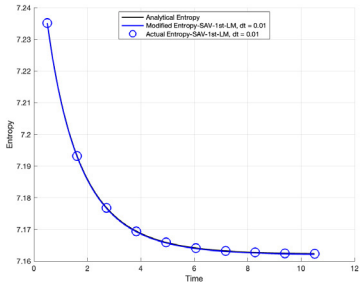

(d) Entropy evolution with $\Delta t = 0.01$.

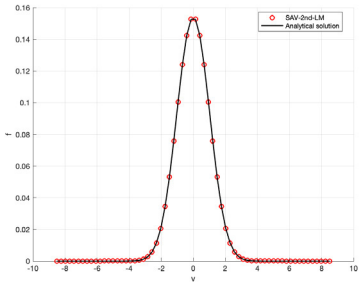

(e) f at $t_{\text{end}} = 10.5$ with $\Delta t = 0.2$.

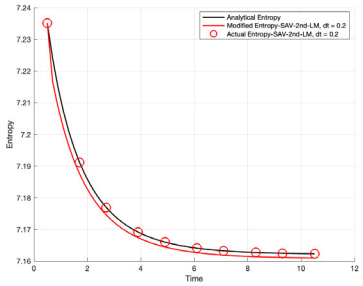

(f) Entropy evolution with $\Delta t = 0.2$.

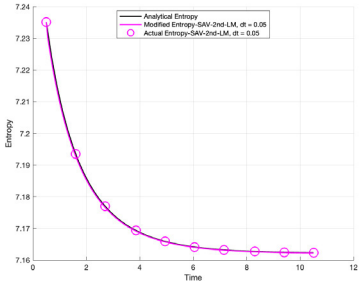

(g) Entropy evolution with $\Delta t = 0.05$.

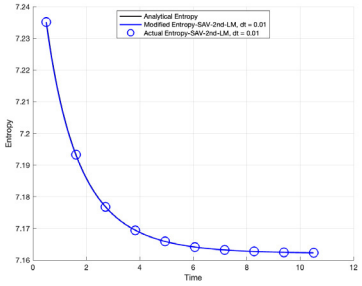

(h) Entropy evolution with $\Delta t = 0.01$.

FIG. 3. *Solution profiles and entropy evolution for the Boltzmann equation with different time step sizes. Top* four *figures:* `SAV-1st-LM`. *Bottom* four *figures:* `SAV-2nd-LM`.

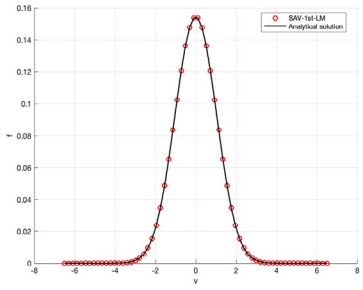

(a) f at $t_{\text{end}} = 10.5$ with $\Delta t = 0.0041$.

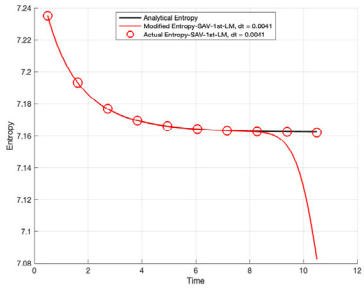

(b) Entropy evolution with $\Delta t = 0.0041$.

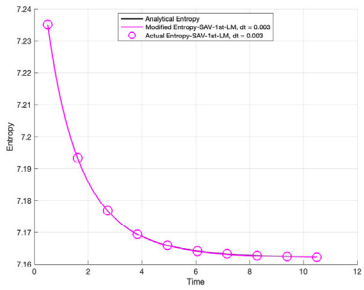

(c) Entropy evolution with $\Delta t = 0.003$.

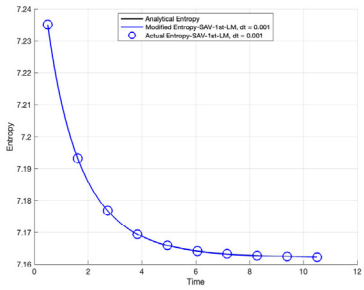

(d) Entropy evolution with $\Delta t = 0.001$.

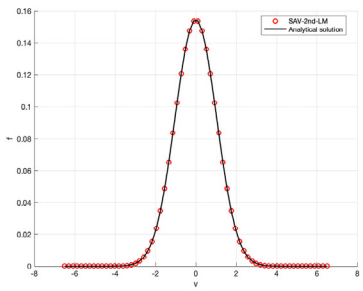

(e) f at $t_{\text{end}} = 10.5$ with $\Delta t = 0.0035$.

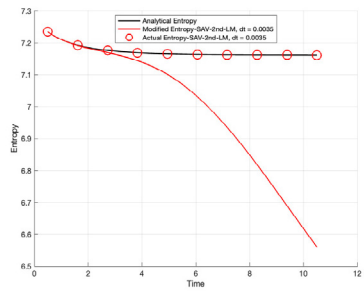

(f) Entropy evolution with $\Delta t = 0.0035$.

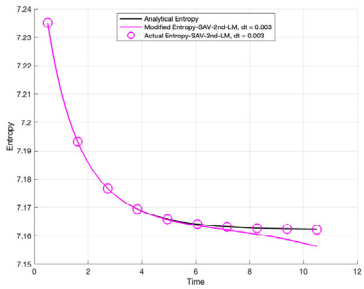

(g) Entropy evolution with $\Delta t = 0.003$.

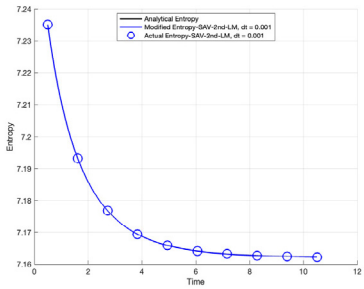

(h) Entropy evolution with $\Delta t = 0.001$.

FIG. 4. *Solution profiles and entropy evolution for the Landau equation with different time step sizes. Top* four *figures:* `SAV-1st-LM`. *Bottom four figures:* `SAV-2nd-LM`.

actual entropy, it often indicates that the positivity and mass conservation correction is triggered, in which case `SAV-1st` and `SAV-2nd` will fail. For larger time step sizes, the modified entropy decays faster than the actual entropy, but the actual entropy always matches closely the analytical entropy.

Generally speaking, when using the SAV schemes with a sufficiently small time step size, the modified entropy will closely match the actual entropy. For larger time step sizes, the modified entropy is likely to decay at a faster rate than the actual entropy. This accelerated decay of the modified entropy contributes to stabilizing the scheme, enabling the actual entropy generated by the SAV schemes to closely approximate the true entropy.

5.1.4. Positivity-preserving SAV scheme for the Boltzmann equation. We now examine the performance of the first order positivity-preserving SAV scheme, `SAV-1st-P-B`, for solving the Boltzmann equation.

For this scheme to be positive, the parameter β is required to be larger than $\frac{r^0}{\sqrt{H_{\min}}} \max Q_B^-(f)$, where $r^0 = 2.6898$, $\sqrt{H_{\min}} \approx 2.6780$, and $\max Q_B^-(f) = 1$ in the BKW test. Therefore, β is chosen as 1.1, 5, 10, and 100. We first perform a convergence test using time step sizes of $\Delta t = 0.2, 0.1, 0.05,$ and 0.025. For each time step size, we run the solution to $t_{\text{end}} = 2.5$ and evaluate the relative L_∞ error between the numerical solution and the analytical one. The results are shown in Figure 5a, from which we observe the expected first order convergence. It is also clear that larger β results in larger error in magnitude. So in practice, β should be chosen as close as possible to the required lower bound. We then fix the time step size $\Delta t = 0.025$ and plot the entropy evolution for different values of β in Figure 5b. The modified entropy always matches well the actual entropy. However, larger β results in larger deviation from the analytical entropy, so the proper choice of β is also critical to obtain a correct entropy dissipation rate.

5.2. Test case 2. In this test, we consider the following initial condition

$$f^0(v) = \frac{\rho_1}{2\pi T_1} \exp\left(-\frac{|v - V_1|^2}{2T_1}\right) + \frac{\rho_2}{2\pi T_2} \exp\left(-\frac{|v - V_2|^2}{2T_2}\right), \tag{5.2}$$

with $\rho_1 = \rho_2 = 1/2$, $T_1 = T_2 = 1$, and $V_1 = (-1, 2)$, $V_2 = (3, -3)$. For the Boltzmann equation, S is set to 5; and for the Landau equation, S is set to 7.5. For this initial condition, we don't know the analytical solution**,** but we do know that the solution will relax to the Maxwellian after a long time.

In Figure 6, we illustrate the evolution of the distribution function for both the Boltzmann equation (with $\Delta t = 0.01$) and Landau equation (with $\Delta t = 0.002$) from initial time $t_0 = 0$ to final time $t_{\text{end}} = 10$, computed using `SAV-2nd-LM`. The expected trend of the solution is observed. In Figure 7, we compared the modified entropy against the actual entropy obtained. The results demonstrate a consistent alignment between the modified and actual entropy, highlighting the ability of the proposed scheme to capture the entropy dissipation structure.

Furthermore, we examine the conservation properties of the `SAV-2nd-LM` scheme. For both the Boltzmann and Landau equations, we plot in Figure 8 the evolution of the absolute errors in mass, momentum (first component) and energy relative to their initial values. The results clearly show that mass is conserved to machine precision. In contrast, momentum and energy are not as well conserved over the long term, as

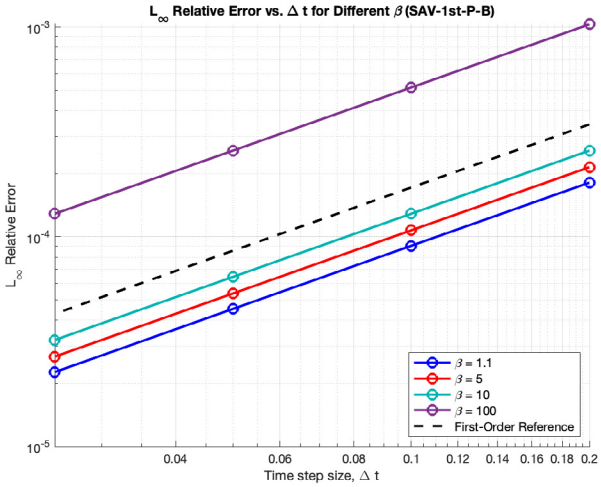

(a) Convergence test of the `SAV-1st-P-B` scheme for different values of β ($\beta = 1.1, 5, 10, 100$) and $\Delta t = 0.2, 0.1, 0.05, 0.025$.

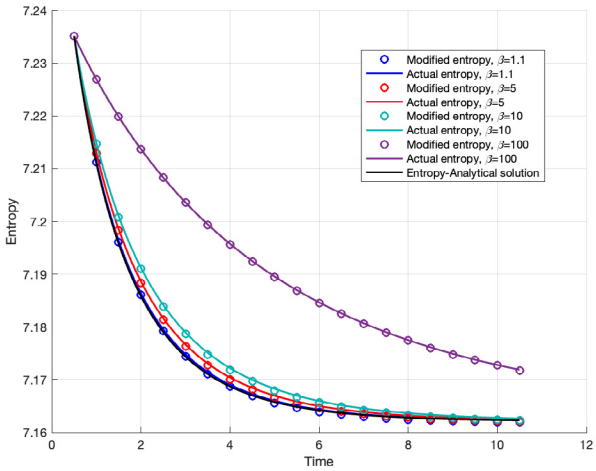

(b) Comparison of the modified entropy and actual entropy of the `SAV-1st-P-B` scheme, and the analytical entropy for different values of β ($\beta = 1.1, 5, 10, 100$) and a fixed time step size $\Delta t = 0.025$.

FIG. 5. *Convergence test and entropy evolution of the `SAV-1st-P-B` scheme.*

the scheme does not strictly enforce them. If desired, they can be preserved using a similar strategy as mentioned in Remark 4.5.

6. Conclusions. We developed novel numerical schemes to tackle the dual challenge of enabling entropy dissipation and preserving positivity for general kinetic equations, leveraging the recently introduced SAV approach. Both the first order

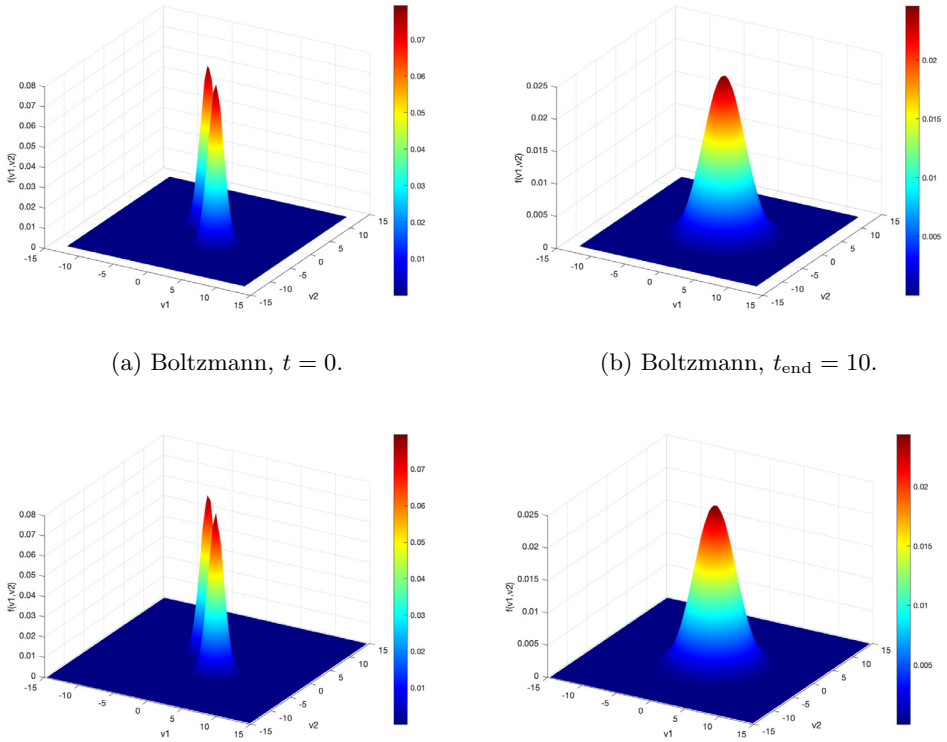

(a) Boltzmann, $t = 0$. (b) Boltzmann, $t_{\text{end}} = 10$.

(c) Landau, $t = 0$. (d) Landau, $t_{\text{end}} = 10$.

FIG. 6. *Initial ($t = 0$) and final ($t_{end} = 10$) solution profiles, computed using the* `SAV-2nd-LM` *scheme. Top row: Boltzmann equation ($\Delta t = 0.01$). Bottom row: Landau equation ($\Delta t = 0.002$).*

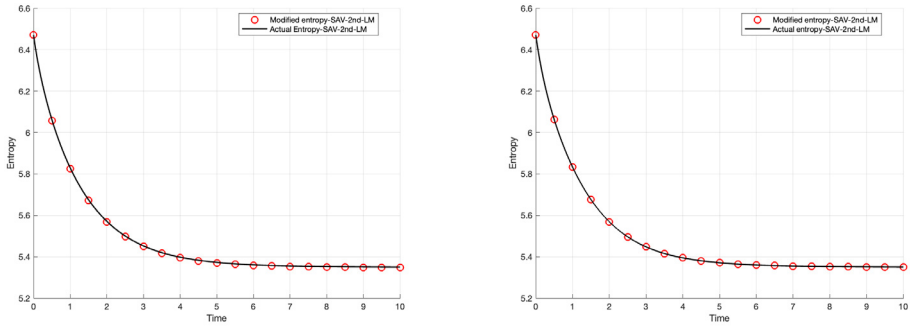

(a) Boltzmann equation. (b) Landau equation.

FIG. 7. *Entropy evolution computed using the* `SAV-2nd-LM` *scheme. The plots show the agreement between the modified SAV entropy and the actual entropy for both the Boltzmann ($\Delta t = 0.01$) and Landau ($\Delta t = 0.002$) equations.*

and second order schemes were constructed. We applied the proposed schemes to the nonlinear Boltzmann equation and Landau equation, which are among the most challenging kinetic equations, and presented convincing numerical results which

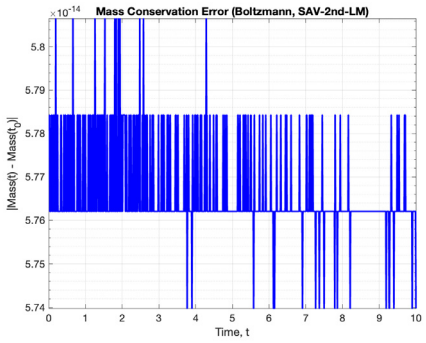

(a) Mass error (Boltzmann).

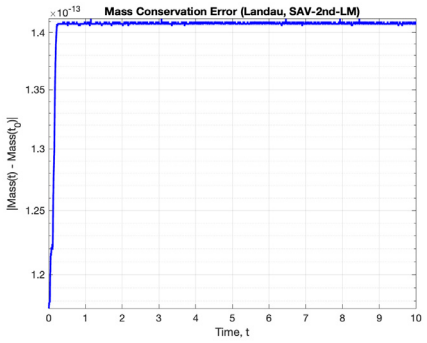

(b) Mass error (Landau).

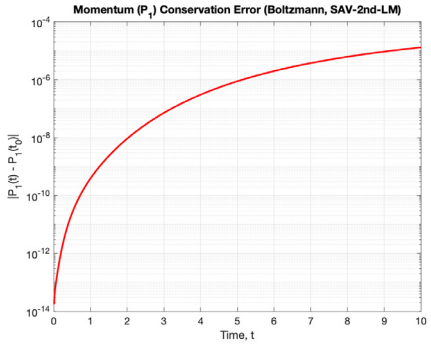

(c) Momentum error (Boltzmann).

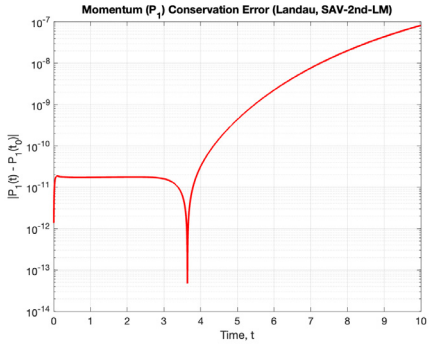

(d) Momentum error (Landau).

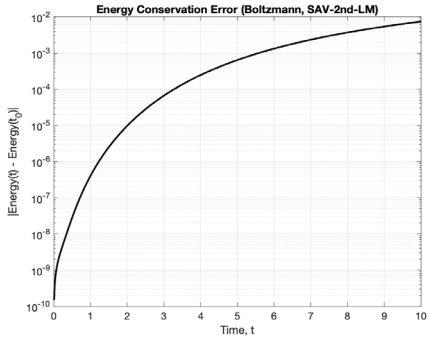

(e) Energy error (Boltzmann).

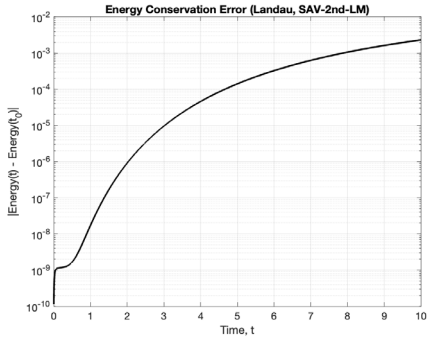

(f) Energy error (Landau).

FIG. 8. *Time evolution of the errors in mass, momentum, and energy of the* `SAV-2nd-LM` *scheme. The left column shows results for the Boltzmann equation (with* $\Delta t = 0.01$*), and the right column shows results for the Landau equation (with* $\Delta t = 0.002$*).*

showed that the proposed schemes are both robust and efficient. Future work includes the extension of these schemes to treat the spatially inhomogeneous kinetic equations.

REFERENCES

[1] X. Antoine, J. Shen, and Q. Tang, *Scalar auxiliary variable/Lagrange multiplier based pseudospectral schemes for the dynamics of nonlinear Schrödinger/Gross–Pitaevskii equations*, J. Comput. Phys., 437 (2021), 110328, https://doi.org/10.1016/j.jcp.2021.110328.

[2] M. Bergounioux, K. Ito, and K. Kunisch, *Primal-dual strategy for constrained optimal control problems*, SIAM J. Control Optim., 37 (1999), pp. 1176–1194, https://doi.org/10.1137/S0363012997328609.

[3] P. L. Bhatnagar, E. P. Gross, and M. Krook, *A model for collision processes in gases.* I. *Small amplitude processes in charged and neutral one-component systems*, Phys. Rev., 94 (1954), pp. 511–525, https://doi.org/10.1103/PhysRev.94.511.

[4] J. C. Butcher, *Numerical Methods for Ordinary Differential Equations*, John Wiley & Sons, 2016.

[5] Z. Cai, J. Hu, Y. Kuang, and B. Lin, *An entropic method for discrete systems with Gibbs entropy*, SIAM J. Numer. Anal., 60 (2022), pp. 2345–2371, https://doi.org/10.1137/21M1429023.

[6] C. Cercignani, *The Boltzmann Equation and Its Applications*, Springer-Verlag, New York, 1988.

[7] Q. Cheng and J. Shen, *Multiple scalar auxiliary variable (MSAV) approach and its application to the phase-field vesicle membrane model*, SIAM J. Sci. Comput., 40 (2018), pp. A3982–A4006, https://doi.org/10.1137/18M1166961.

[8] Q. Cheng and J. Shen, *A new Lagrange multiplier approach for constructing structure preserving schemes,* I. *Positivity preserving*, Comput. Methods Appl. Mech. Engrg., 391 (2022), 114585, https://doi.org/10.1016/j.cma.2022.114585.

[9] P. Degond and B. Lucquin-Desreux, *An entropy scheme for the Fokker–Planck collision operator of plasma kinetic theory*, Numer. Math., 68 (1994), pp. 239–262, https://doi.org/10.1007/s002110050059.

[10] G. Dimarco and L. Pareschi, *Numerical methods for kinetic equations*, Acta Numer., 23 (2014), pp. 369–520, https://doi.org/10.1017/S0962492914000063.

[11] C. M. Elliott and A. Stuart, *The global dynamics of discrete semilinear parabolic equations*, SIAM J. Numer. Anal., 30 (1993), pp. 1622–1663, https://doi.org/10.1137/0730084.

[12] D. J. Eyre, *Unconditionally gradient stable time marching the Cahn–Hilliard equation*, MRS Online Proceedings Library (OPL), 529 (1998), 39, https://doi.org/10.1557/PROC-529-39.

[13] F. Facchinei and J.-S. Pang, *Finite-dimensional Variational Inequalities and Complementarity Problems*, Springer, 2003.

[14] I. Gamba, J. Haack, C. Hauck, and J. Hu, *A fast spectral method for the Boltzmann collision operator with general collision kernels*, SIAM J. Sci. Comput., 39 (2017), pp. B658–B674, https://doi.org/10.1137/16M1096001.

[15] P. T. Harker and J.-S. Pang, *Finite-dimensional variational inequality and nonlinear complementarity problems: A survey of theory, algorithms and applications*, Math. Program., 48 (1990), pp. 161–220, https://doi.org/10.1007/BF01582255.

[16] L. Holway, *Kinetic theory of shock structure using an ellipsoidal distribution function*, in Proceedings of the 4th International Symposium on Rarefied Gas Dynamics, Vol. I, Academic Press, New York, 1966, pp. 193–215.

[17] K. Ito and K. Kunisch, *Lagrange Multiplier Approach to Variational Problems and Applications*, SIAM, 2008.

[18] L. D. Landau, *The kinetic equation in the case of Coulomb interaction*, Zh. Eksper. i Teoret. Fiz., 7 (1937), pp. 203–209.

[19] L. Lin, Z. Yang, and S. Dong, *Numerical approximation of incompressible Navier-Stokes equations based on an auxiliary energy variable*, J. Comput. Phys., 388 (2019), pp. 1–22, https://doi.org/10.1016/j.jcp.2019.03.012.

[20] X. Liu, J. Shen, and X. Zhang, *An efficient and robust scalar auxialiary variable based algorithm for discrete gradient systems arising from optimizations*, SIAM J. Sci. Comput., 45 (2023), pp. A2304–A2324, https://doi.org/10.1137/23M1545744.

[21] Z. Liu, Y. Zhang, and X. Li, *A Novel Energy-Optimal Scalar Auxiliary Variable (EOP-SAV) Approach for Gradient Flows*, preprint, arXiv:2304.11288, 2023.

[22] C. Lu, W. Huang, and E. S. Van Vleck, *The cutoff method for the numerical computation of nonnegative solutions of parabolic PDEs with application to anisotropic diffusion and lubrication-type equations*, J. Comput. Phys., 242 (2013), pp. 24–36, https://doi.org/10.1016/j.jcp.2013.01.052.

[23] Z. Ma, Z. Mao, and J. Shen, *Efficient and stable SAV-based methods for gradient flows arising from deep learning*, J. Comput. Phys., 505 (2024), 112911, https://doi.org/10.1016/j.jcp.2024.112911.
[24] C. Mouhot and L. Pareschi, *Fast algorithms for computing the Boltzmann collision operator*, Math. Comp., 75 (2006), pp. 1833–1852, https://doi.org/10.1090/S0025-5718-06-01874-6.
[25] L. Pareschi and G. Russo, *Numerical solution of the Boltzmann equation* I*: Spectrally accurate approximation of the collision operator*, SIAM J. Numer. Anal., 37 (2000), pp. 1217–1245, https://doi.org/10.1137/S0036142998343300.
[26] L. Pareschi, G. Russo, and G. Toscani, *Fast spectral methods for the Fokker–Planck–Landau collision operator*, J. Comput. Phys., 165 (2000), pp. 216–236, https://doi.org/10.1006/jcph.2000.6612.
[27] J. Shen, C. Wang, X. Wang, and S. M. Wise, *Second-order convex splitting schemes for gradient flows with Ehrlich–Schwoebel type energy: Application to thin film epitaxy*, SIAM J. Numer. Anal., 50 (2012), pp. 105–125, https://doi.org/10.1137/110822839.
[28] J. Shen and J. Xu, *Convergence and error analysis for the scalar auxiliary variable (SAV) schemes to gradient flows*, SIAM J. Numer. Anal., 56 (2018), pp. 2895–2912, https://doi.org/10.1137/17M1159968.
[29] J. Shen, J. Xu, and J. Yang, *The scalar auxiliary variable (SAV) approach for gradient flows*, J. Comput. Phys., 353 (2018), pp. 407–416, https://doi.org/10.1016/j.jcp.2017.10.021.
[30] J. Shen, J. Xu, and J. Yang, *A new class of efficient and robust energy stable schemes for gradient flows*, SIAM Rev., 61 (2019), pp. 474–506, https://doi.org/10.1137/17M1150153.
[31] J. J. van der Vegt, Y. Xia, and Y. Xu, *Positivity preserving limiters for time-implicit higher order accurate discontinuous Galerkin discretizations*, SIAM J. Sci. Comput., 41 (2019), pp. A2037–A2063, https://doi.org/10.1137/18M1227998.
[32] C. Villani, *Fisher information estimates for Boltzmann's collision operator*, J. Math. Pures Appl., 77 (1998), pp. 821–837, https://doi.org/10.1016/S0021-7824(98)80010-X.
[33] C. Villani, *A review of mathematical topics in collisional kinetic theory*, in Handbook of Mathematical Fluid Mechanics, Vol. I, S. Friedlander and D. Serre, eds., North-Holland, 2002, pp. 71–305.
[34] J. Zhang, S. Zhang, J. Shen, and G. Lin, *Energy-dissipative evolutionary deep operator neural networks*, J. Comput. Phys., 498 (2024), 112638, https://doi.org/10.1016/j.jcp.2023.112638.
[35] S. Zhang and J. Shen, *Structure preserving schemes for a class of Wasserstein gradient flows*, Commun. Appl. Math. Comput., 7 (2025), pp. 1174–1194, https://doi.org/10.1007/s42967-025-00486-2.
[36] S. Zhang, J. Zhang, J. Shen, and G. Lin, *A relaxed vector auxiliary variable algorithm for unconstrained optimization problems*, SIAM J. Sci. Comput., 47 (2025), pp. C126–C150, https://doi.org/10.1137/23M1611087.